Biofabrication

PAPER

Three-dimensional bioprinting of complex cell laden alginate hydrogel structures

Atabak Ghanizadeh Tabriz[1,2], **Miguel A Hermida**[1], **Nicholas R Leslie**[1] **and Wenmiao Shu**[1,2]

[1] Institute of Biological Chemistry, Biophysics and Bioengineering, School of Engineering and Physical Sciences, Heriot-Watt University, Edinburgh EH14 4AS, UK

[2] Institute of Mechanical, Process and Energy Engineering, School of Engineering and Physical Sciences, Heriot-Watt University, Edinburgh EH14 4AS, UK

E-mail: w.shu@hw.ac.uk

Keywords: 3D bioprinting, alginate hydrogel, cell viability, stability, rigidity, sterilization

OPEN ACCESS

RECEIVED
21 July 2015

REVISED
27 November 2015

ACCEPTED FOR PUBLICATION
3 December 2015

PUBLISHED
22 December 2015

Abstract

Different bioprinting techniques have been used to produce cell-laden alginate hydrogel structures, however these approaches have been limited to 2D or simple three-dimension (3D) structures. In this study, a new extrusion based bioprinting technique was developed to produce more complex alginate hydrogel structures. This was achieved by dividing the alginate hydrogel cross-linking process into three stages: primary calcium ion cross-linking for printability of the gel, secondary calcium cross-linking for rigidity of the alginate hydrogel immediately after printing and tertiary barium ion cross-linking for long-term stability of the alginate hydrogel in culture medium. Simple 3D structures including tubes were first printed to ensure the feasibility of the bioprinting technique and then complex 3D structures such as branched vascular structures were successfully printed. The static stiffness of the alginate hydrogel after printing was 20.18 $\pm$ 1.62 KPa which was rigid enough to sustain the integrity of the complex 3D alginate hydrogel structure during the printing. The addition of 60 mM barium chloride was found to significantly extend the stability of the cross-linked alginate hydrogel from 3 d to beyond 11 d without compromising the cellular viability. The results based on cell bioprinting suggested that viability of U87-MG cells was 93 $\pm$ 0.9% immediately after bioprinting and cell viability maintained above 88% $\pm$ 4.3% in the alginate hydrogel over the period of 11 d.

1. Introduction

In the past decade, three-dimension (3D) bioprinting as an emerging new technology for tissue engineering has made significant progress towards the regeneration of transplantable tissues [1–3] and even organs such as human ear, bones, skins, nose [4–7] for restoring or repairing the damaged body functions. Different biofabrication techniques including inkjet printing [8–13] bioextrusion [14–16] valvejet printing [17–20], laser based printing [21–25] and photopolymerization [26, 27] have been developed for the 3D printing of live cells and bioscaffolds. However, although the fabrication of clinically scaled hard tissues such as bones have already been successfully demonstrated [6], the bioprinted scaffolds for soft tissues are currently limited to clinically small scale structures with limited complexity.

The key challenge has been the difficulty of striking a good balance between the conditions for printing highly viable cells and producing sufficiently strong scaffold to support clinical scale cell-laden structures at the same time. Take bioextrusion of hydrogels for example, small-diameter nozzles and highly viscous hydrogel materials are desirable to achieve a good printing resolution with sufficient mechanical rigidity for building 3D hydrogel structures. But the higher extrusion forces needed to print highly viscous materials from a small nozzle will lead to higher shear stresses and hence reduced cell viability during the printing process. To overcome this key challenge, different bioprinting approaches have been developed. Butcher and co-workers [28] developed a novel ultraviolet (UV) bioextrusion printing technique for complex 3D structures. Living cells in an UV curable, low-viscosity PEG hydrogel solution are printed with *in situ* UV

radiation to solidify the printed hydrogel constructs layer by layer. As the hydrogel is cross-linked after the cells are extruded from the printing nozzle, this technique is able to significantly reduce the shear stress associated with printing high-viscosity hydrogels and produce sufficiently strong UV cross-linked structures for the regeneration of a clinical-scale human heart valve. The requirement of this approach, though, is the need for photosensitive hydrogel materials and the exposure of live cells to potentially harmful UV radiation and toxic photo-initiators. On the other hand, more rigid poly (ε-caprolactone) PCL as a biodegradable scaffold [29] or high dense fluid oil [30] was used to support soft cell laden hydrogels. The use of such hybrid plastic and hydrogel scaffolds enables bioprinting of organ size structures like a human ear [29]. However the need for high temperature printing and acid producing degradation of PCL may limit their application for tissue regeneration. Alternatively, lowering the temperature of hydrogels in printing enhances mechanical rigidity before the gels are cross-linked, leading to alginate-gelatin constructs that have shown the ability to support tumour growth [31, 32] and the formation of highly uniform embryonic stem cell culture in 3D [33].

In this study, we present a new bioprinting technique for complex 3D alginate hydrogel structures with living tumour cells *in vitro*. Alginate hydrogels are chosen as they are probably the most widely used biomaterials in 3D bioprinting because of its biocompatibility, reversible control over stiffness and capability to form highly porous structures for cell regeneration. To validate the new 3D bioprinting technology, we chose U87-MG cell line which is an established human brain tumour cell line for cancer disease models with fully genetic characterisation [34–37]. 3D bioprinting of cell-laden alginate hydrogels will be demonstrated for complex structures such as clinically sized branched vascular structures. The mechanical properties as well as the degradation time of the printed alginate hydrogel structures are also assessed before and after printing. In addition, post-printing cell viability was assessed over 11 d period.

2. Materials and methods

2.1. Materials and reagents

In this study, sodium alginate 8% w/v (Product number W201502, Sodium Alginate, Sigma-Aldrich, Gillingham, UK), $CaCl_2$ solution (Product number 223506 $CaCl_2$ dehydrate, Sigma-Aldrich, Gillingham, UK) and $BaCl_2$ Solution (Product number 1001253915 $BaCl_2$ trace metals basis, Sigma-Aldrich, Gillingham, UK) were prepared in deionised water at room temperature. In addition an ultra-sonic bath set at 60 °C was used to reduce the mixing time of sodium alginate with deionised water to produce homogenous solution overnight. 80 mM $CaCl_2$, 100 mM $CaCl_2$ and 60 mM $BaCl_2$ were used respectively as primary, secondary and tertiary cross-linking agents for 8% w/v sodium alginate.

2.2. Partially cross-linked alginate hydrogel preparation

Sodium alginate 8% w/v was sterilised by Gamma radiation (IBL-637 CIS-BioINternational gamma irradiator, France) for 10 Gy at the rate of 1 Gy min^{-1}. 80 mM $CaCl_2$ stocks were autoclaved at 121 °C for 15 min. The two solutions consisting of 8% w/v sodium alginate and 80 mM $CaCl_2$ were mixed with a volume ratio of 1:1 to result a partially cross-linked hydrogel in a 50 ml conical tube (Centrifuge tube, Fisher Scientific Ltd, Loughborough, UK). The hydrogel solution was further mixed using a vortex mixer at room temperature at 1500 rpm for 30 s in order to get the homogeneously partially cross-linked alginate hydrogel.

2.3. Cell culture and transduction

Human glioma U87-MG cells, originally purchased from European Collection of Cell Cultures (Public Health England, UK), were seeded at the density of 0.5×10^6 ml^{-1} in six-well plates and were allowed to attach and acquire normal morphology. Then the cells were transduced using a lentiviral vector which expresses enhanced green fluorescent protein under control of the SFFV promoter. After transduction, cells were seeded in 96-well plates at a cell density of 0.7 cells per well, allowing the selection of a single transduced cell population which were replicated for 2 weeks until a stable clone EGFP1-U87-MG (U87-MG) line was generated. U87-MG cells were cultured in minimum essential medium supplemented with 10% (v/v) foetal bovine serum, L-Glutamine, non-essential amino acids, and sodium pyruvate. All culture medium components were from Life Technologies. During experimental procedures, medium was supplemented with penicillin/streptomycin (100 UI ml^{-1} and 100 μg ml^{-1}). After printing, cells were maintained at 37 °C and with 5% CO_2 in 10 cm petri dishes (Fisher Scientific, UK). The culture media were changed every 2 d.

2.4. Development of bioprinting platform

A modified version of an open source Fab@Home model dual syringe extrusion-based 3D printer was used as the main printing platform for the alginate hydrogel. It consists of an automated *X*–*Y*–*Z* stage where the positioning precision is 100 μm. With its dual switchable dispensing system, it is capable of printing with precision down to 100 μm in *X*–*Y* plane as well as printing with a precision of 100 μm in *Z* plane. Fab@Home models have previously been used to print alginate hydrogel and other biomaterials such as gelatine [38, 39]. A modified new *z* axis carriage figure 1(a) was designed and put in place to enable

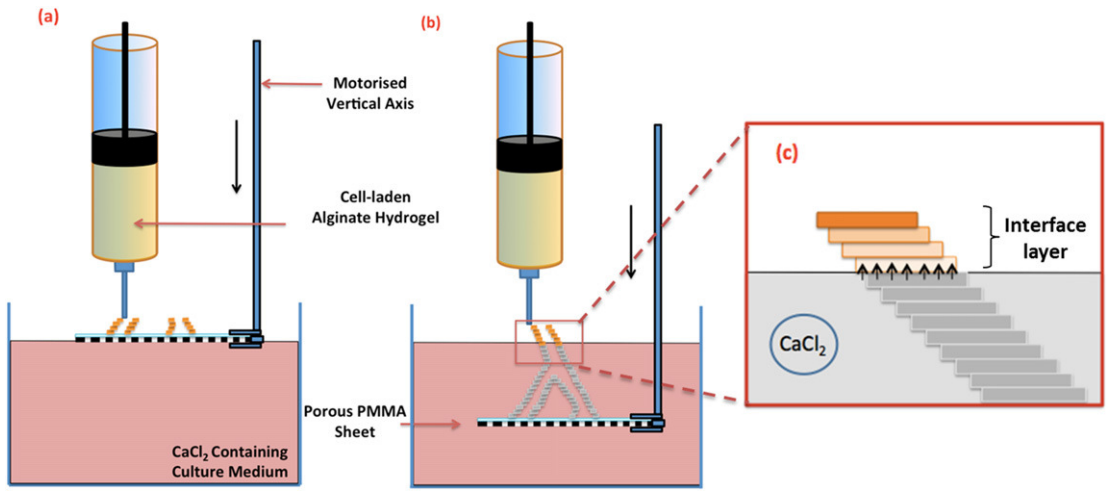

Figure 1. Schematic drawing of the alginate hydrogel 3D printing setup. (a) First few layers of partially cross-linked alginate hydrogel were initially printed on the porous membrane where at this stage the structure was able to support its shape. (b) Further cross-linking of the hydrogel once the *Z* axis was lowered down and the printed partially cross-linked alginate hydrogel were submerged into the $CaCl_2$ bath which creates a better support for the upcoming layers. (c) The interface layers: upward diffusion of Ca^{+2} ions into the interface layers which are partially cross-linked above the $CaCl_2$ solution.

merging the *Z* platform into a 100 mM $CaCl_2$ solution bath as the secondary cross-linking reagent to further cross-link the printed partially cross-linked alginate hydrogel. Initially the first few layers of partially cross-linked alginate hydrogel will be printed above the $CaCl_2$ solution on a porous nitrocellulose membrane. The membrane assures the appropriate adhesion of the partially cross-linked hydrogel to the surface for better support while allowing $CaCl_2$ solution diffusing into the structure for cross-linking. The porous membrane is connected to a thin Poly methyl methacrylate sheet with pore sizes of 0.8 mm to allow $CaCl_2$ to enter the inner sections of the printed structures. The *z*-axis will be lowered down leading to the first printed layers submerging into the $CaCl_2$ solution for further cross-linking shown in figure 1(b), the subsequent printing of the alginate hydrogel was supported by the partially cross-linked hydrogel structures above the solution. Diffusion would also enable $CaCl_2$ solution to penetrate inside the hallow sections of the printed layers as well as the layers that are being printed above the $CaCl_2$ solution, forming an interface layer where rigidity of the hydrogel layers was sufficient enough to support a few layers of printed hydrogel structures. By repeating this sequential printing process, a complete 3D structure can be generated. Once the printing process was complete, the structure was exposed to 60 mM of $BaCl_2$ as the tertiary cross-linking procedure for 2 min.

2.5. Design and 3D printing of alginate hydrogel structures

3D printed structures were designed using the CAD programme Solid Edge V20. Vascular structure design was extracted from an online open source GrabCAD 3D CAD library. The CAD files were then converted to stl files and transferred to the relative software to generate printing paths. The partially cross-linked alginate hydrogel was loaded into the extrusion syringes and then nozzles with 0.33 mm ID or 0.51 mm ID (TE series Nozzles, OK International, Hampshire, UK) fitted to the end of syringes. The printing path width was 0.35 mm and 0.55 mm respectively as well as printing height of 0.3 and 0.475 mm. The printing speed was 6 mm s^{-1} which was ideal for both set of nozzles. Extrusion speed was to be set as 0.45 ml min^{-1} and 0.65 ml min^{-1} respectively.

2.6. Viscosity measurements of partially cross-linked alginate hydrogels and their printibility.

Sodium alginates at concentrations of 1%, 2%, 3%, 4%, 5%, 6%, 7%, 8%, 9%, 10%, 11% and 12% (w/v) were mixed with $CaCl_2$ Solutions at concentrations of 10 mM, 20 mM, 30 mM, 40 mM, 50 mM, 60 mM, 70 mM, 80 mM, 90 mM, 100 mM, 110 mM and 120 mM respectively at volume ratio of 1:1 to partially cross-link the sodium alginate. Different range of partially cross-linked alginate hydrogels were printed into 20 mm × 20 mm × 2 mm structures to find the optimum hydrogel concentration with self-support ability. The viscosity profile measurement of each partially cross-linked alginate hydrogel was carried out by Bohlin Gemini rheometer (Malvern Instruments).

2.7. Mechanical testing

The partially cross-linked alginate hydrogel was printed by exposure to 50 mM, 100 mM, 200 mM and 300 mM $CaCl_2$ solutions respectively to generate cubic structures with dimensions of 20 mm × 20 mm × 8 mm. They were kept in the solution for 10 min followed by the exposure to 60 mM $BaCl_2$ solution for

2 min. Mach-1™ mechanical indenter (Biomomentum, Canada) was used to measure the static stiffness. The partially cross-linked alginate hydrogel was also mechanically tested before printing to understand the significant effect of $CaCl_2$ in order to enhance the mechanical properties of the gel.

2.8. Cell laden alginate hydrogel solution for printing

2 ml of 8% w/v sodium alginate initially was loaded with 1 ml of U87-MG cell suspension at a concentration of 21×10^6 ml^{-1} in the extrusion syringe. The solution was then mixed with 1 ml of 160 mM $CaCl_2$ to partially cross-link the hydrogel using a vortex mixer at 1200 rpm for 30 s at room temperature. The cell laden alginate solution had final concentrations of 4% w/v alginate and 5.25×10^6 ml^{-1} cells.

2.9. Live and dead cell assay

For the visualisation of dead cells in the hydrogel, propidium iodide (PI, Sigma Aldrich UK) was added directly to the media in the 10 cm Petri dishes (Fisher Scientific, UK) containing the constructs at a final concentration of 2.5 μM. After 30 min incubation in the dark at 37 °C, the culture media was removed and the coverslips (Cover Glass, 631-0152, VWR International USA) containing the hydrogel were mounted in microscope slides to proceed for imaging.

2.10. MTT assay

Cell number was assessed using (3-(4,5-Dimethylthiazol-2-yl)-2,5-diphenyltetrazolium bromide (MTT). U87-MG cells were seeded in a 96 well plate at 7.5×10^4 cells ml^{-1} and incubated overnight. Cells were then exposed to different conditions during this time and number of metabolically active cells was estimated after 24 h by measuring absorbance at 570 nm. Each condition was determined using triplicates.

2.11. 3D Cell imaging and viability test

Confocal laser scanning microscopy (Leica SP5 SMD; Leica microsystems) was used for image acquisition. Images were taken using a dry 20X objective. CLSM images were analysed using Imaris software to investigate the viability of the bioprinted cells over 11 d. Cell viability of the bioprinted structures at 2%, 3%, 4%, 5% and 6% of the partially cross-linked alginate concentrations (w/v) was assessed after bioprinting.

3. Results and discussions

3.1. Development to partially cross-link alginate hydrogel and its printibility

The key working principle of the new bioprinting method is the ability to print alginate hydrogels with sufficiently high viscosity so that the printed structure can self-support and form an interface layer. In this way, new layers of fresh partially cross-linked alginate hydrogel can be printed onto a relatively solid substrate or the interface layer above the cross-linking reagent bath to build the structure layer-by-layer. However, fully cross-linked hydrogel for extrusion would not be suitable because it would require enhanced shear stress for printing with an adverse effect on cell viability, in addition to the poor adhesion between the printed layers. In order to achieve this balance, we developed here the specified concentrations of the alginate and $CaCl_2$ solutions to form partially cross-linked alginate hydrogel designed to achieve suitable mechanical rigidity with sufficiently low viscosity to avoid high printing shear stresses. A range of alginate concentrations (i.e. 1% w/v to 8% w/v) and $CaCl_2$ concentrations (i.e. 10–800 mM) combinations were made to produce the partially cross-linked hydrogel mixture for testing the best printing quality. The composition of 4% alginate and 40 mM $CaCl_2$ was found to be the minimum concentration needed to create the interface layers. However, the suitable ratio to partially cross-linked alginate hydrogel was 10:1 (w/w) of alginate to $CaCl_2$ at 1:1 volume ratio where lower ratios would result in fully cross-linking the alginate and turning into an inhomogeneous gel which is not suitable for bioprinting. In the other hand, higher alginate to $CaCl_2$ ratios might lead to homogenous gel but would decrease the rigidity of the gel due to lower presence of $CaCl_2$ in the gel. Therefore, 10:1 (w/w) of alginate to $CaCl_2$ was fixed for partially cross-linked alginate hydrogels.

In order to fine-tune the optimal conidtions to 3D print partially cross-linked alginate hydrogel, a wide range of alginate hydrogel with relavant cross-linking conditions were prepared and printed as shown in figure 2. Partially cross-linked alginate concentrations from 0.5% up to 2.5% did not exhibit sufficient mechnical strength to self-support the printed structures. Higher concentrations of alginate at 3% and 3.5% could preserve the structure's shape, however the printed structures were too soft to maintain good structural integrity. The minimum alginate concentration which could self-support its structure for good structural integrity was found to be 4% (w/v) with final $CaCl_2$ concentrartion of 40 mM.

3.2. The effect of $CaCl_2$ and $BaCl_2$ cross-linking bath on the mechanical properties of printed hydrogels

The mechanical testing suggested that after the partially cross-linked alginate hydrogel was further cross-linked it will have good elastic behaviour. The elastic modulus was 5.2 ± 0.12 KPa, 20.18 ± 1.62 KPa, 20.87 ± 1.78 KPa and 28.24 ± 0.91 KPa respectively with exposure to 50 mM, 100 mM, 200 mM and 300 mM $CaCl_2$ and followed by exposure to 60 mM $BaCl_2$. The partially cross-linked alginate hydrogel showed an elastic behaviour with elastic modulus of 1.55 ± 0.027 KPa through strain of 1 ± 0.05 mm.

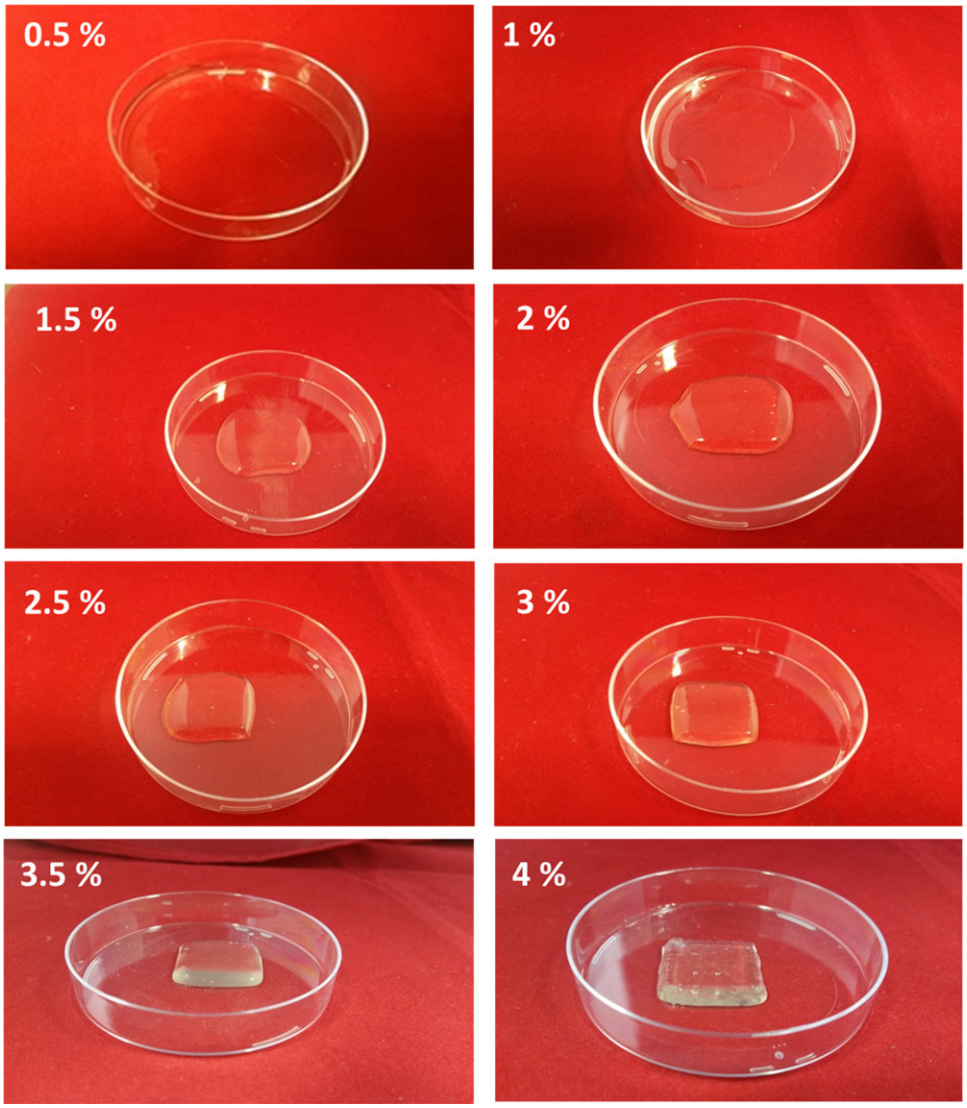

Figure 2. 3D printed structures (20 mm × 20 mm × 2 mm) with different concentrations of partially cross-linked alginate hydrogel with their relevant pre cross-linking reagents.

Therefore the secondary cross-linking process ($CaCl_2$) had a significant effect on boosting the mechanical properties of the alginate hydrogel to create suitable rigidity and strength for the structure to withstand its shape during the bioprinting process. The results shown in figure 3 reveal 50 mM $CaCl_2$ as the secondary cross-linking agent does not have a suitable effect on mechanical properties of the alginate hydrogel suggesting that it will still have similar mechanical properties to the partially cross-linked alginate hydrogel. However 100 mM of $CaCl_2$ resulted in a noticeable change in partially cross-linked alginate hydrogel mechanical properties giving it a suitable rigidity and strengths. The secondary cross-linking agent was kept at 100 mM to prevent exposure of cells to higher concentrations of $CaCl_2$ which possibly could be harmful and affect the cell viability and function. Exposure to 60 mM $BaCl_2$ did not have a significant effect on the mechanical properties of the hydrogel in general (as shown in figure 3). The change in mechanical stiffness upon $BaCl_2$ treatment appeared less obvious when the hydrogel is cross-linked with higher $CaCl_2$ concentration.

3.3. 3D printed alginate structures

Figure 4(a) shows the simple 3D printed alginate hydrogel tubular structures with descending diameters of 20 mm, 15 mm, 10 mm, and 7.50 mm. The tubular structures were printed by 0.33 mm ID nozzle. They were made of eight printed layers with 2.5 mm in height. All tubes had wall thickness of 1.25 ± 0.05 mm as measured by a calliper. Figure 4(b) shows 10 mm diameter 3D printed alginate hydrogel tubular structures with 32, 24, 16, 8 printed layers respectively. The height of these printed structures was found to be 10.20, 7.40, 5.30 and 2.65. This gave the average printing height of 322 ± 11 μm/layer. Furthermore complex 3D structures such as branched vascular structures shown in figures 4(d) and (e) were printed successfully by 0.51 and 0.33 mm ID tips.

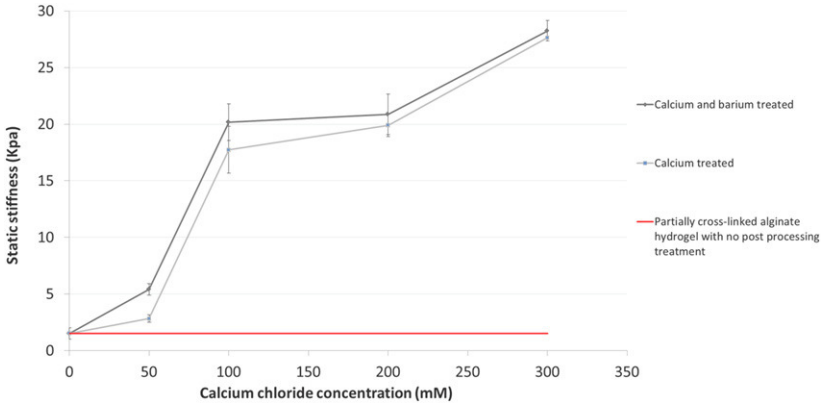

Figure 3. Elastic modulus of partially cross-linked alginate hydrogel exposed to different $CaCl_2$ concentrations for 10 min followed with or without exposure to $BaCl_2$.

Depending upon the complexity of the printed structures the height of the interface layers can be adjusted to ensure the best printing quality. For example for simple 3D structures such as hollow tubes in which the same printing pattern was repeated, the maximum allowable distance of the interface layer from the nozzle tip to $CaCl_2$ bath was found to be 2 mm or four layers for 0.51 mm ID tip and seven layers for 0.33 mm ID tip. Where for complex 3D structures with angular structures it was 0.5 mm or one layer for 0.51 mm ID tip and two layers for 0.33 mm ID tip. The logic behind the shorter distance between the nozzle tip and $CaCl_2$ solution interface for bioprinting complex 3D structures was the lack of suitable mechanical properties of the partially cross-linked alginate hydrogel to support itself when it was printed in an angle. It was noticed that when the nozzle tip was too close to the $CaCl_2$ solution, there were boundaries formed between the printed layers because Ca^{2+} ions could easily diffuse into the printed layers above the $CaCl_2$ bath. However if the nozzle tip is far enough from the $CaCl_2$ bath interface, the printed layers above the $CaCl_2$ solution can merge together more effective and form a more uniform and continuous construct. This new feature provides improved mechanical properties of the alginate hydrogel structures as well as the possibility to bioprint complex structures, which is consistent with the recent finding on continuous 3D printing enabled by Continuous Liquid Interface Production technique [40].

3.4. Degradation of hydrogel and the optimisation of cross-linking conditions

This study was carried out to control and enhance the degradation time of the alginate hydrogel by further cross-linking it with other reagents [41]. $BaCl_2$ solutions at different concentrations were used in order to achieve a suitable degradation time of the alginate hydrogel. The printed grid structures which were exposed to 100 mM of $CaCl_2$ for 10 min and were kept in culture medium (DMEM, 1.8 mM $CaCl_2$) for 7 d shown in figure 5(a). The alginate structure started to break down by the second day and slowly degraded completely after 7 d as expected. By exposure of the alginate hydrogel to 10, 20 and 40 mM of $BaCl_2$ for 2 min after initially being exposed to 100 mM of $CaCl_2$ for 10 min, structural degradation was prevented in accordance with the $BaCl_2$ concentration. However exposure to 10 mM of $BaCl_2$ as shown in figure 5(b) was not enough to keep the printed structure in place over 7 d where the printed grid structure started breaking down day by day but not completely dissolved by day 7. Exposure to 20 mM of $BaCl_2$ as shown in figure 5(c) improved the degradation time of the alginate hydrogel but once again the structure started to crack slowly where presence of any external forces could easily break the grid structure which can cause the cells to escape the alginate structures. However 40 mM $BaCl_2$ as shown in figure 4(d) was able to keep the structure in place over 7 d without the appearance of visible cracks within the grid structure. Based on the alginate hydrogel degradation results, at this stage 40 mM $BaCl_2$ was the minimum concentration needed to be used as tertiary cross-linking agent, however the cell viability needed to be examined to investigate whether the secondary and tertiary cross-linking process had any negative effect.

3.5. The effect of Calcium and Barium concentration on U87-MG Cells

This study was carried out to examine the effects on U87-MG cells from the 100 mM $CaCl_2$ secondary cross-linking reagent and the tertiary cross-linking reagent which was 40 mM $BaCl_2$. U87-MG cells were first treated with 100 mM $CaCl_2$ for 10 min and then exposed to 10 mM, 20 mM, 40 mM, 60 mM and 100 mM $BaCl_2$ respectively for 2 min similar to the printing conditions and then cultured for 24 h. The MTT assay data as shown in figure 6 shows that after 24 h of culture not only are U87-MG cells not affected negatively by exposure to $BaCl_2$ but also the cell growth was seen to be reproducibly improved within

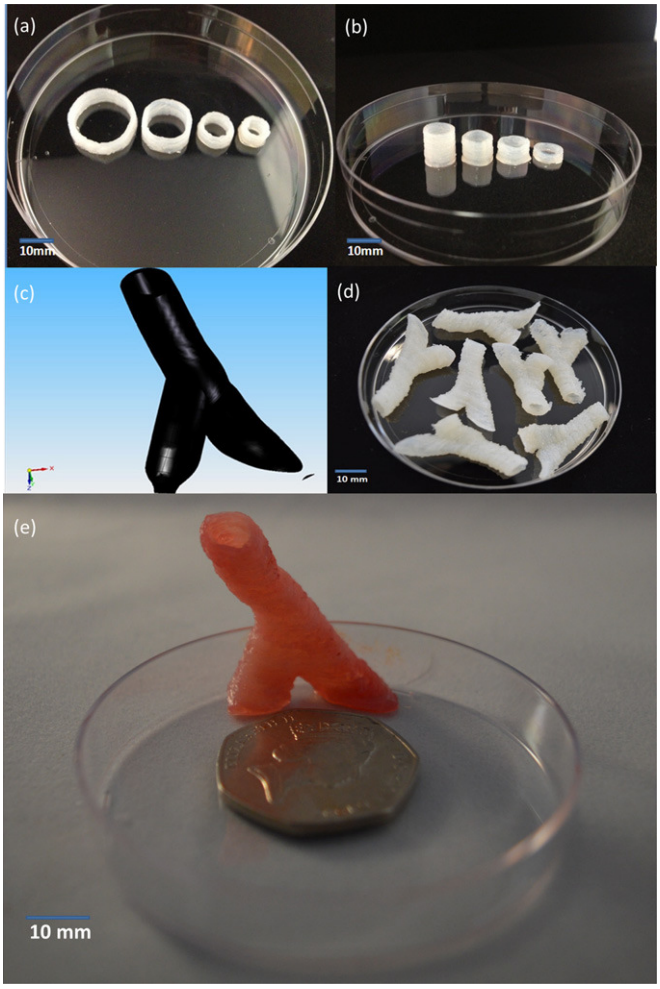

Figure 4. (a) Printed tube structures with descending diameters (b) and descending height. (c) CAD file of the vascular structure in Solid Edge version V20 (d) vascular structures printed by 0.51 mm diameter tip (e) vascular structure printed by 0.33 mm diameter tip.

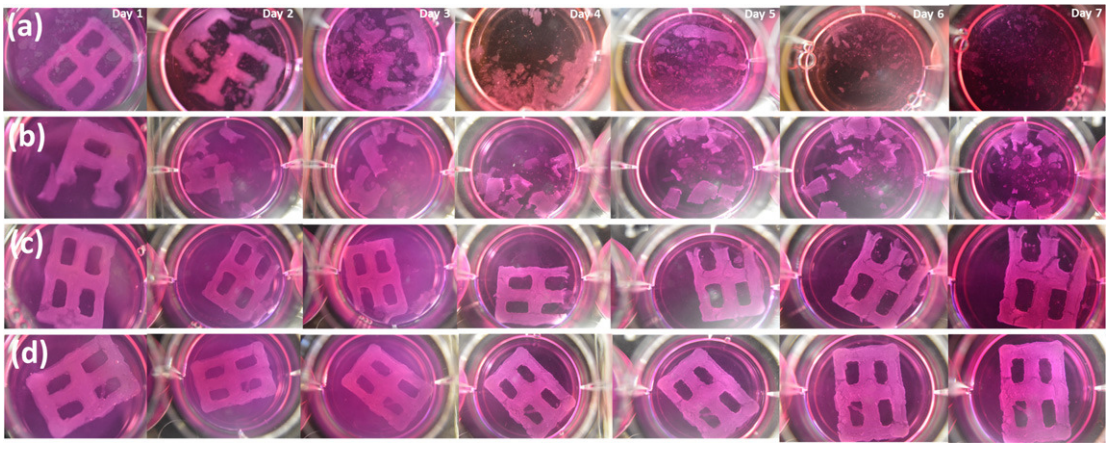

Figure 5. (a) Bioprinted grid structure exposed to 100 mM $CaCl_2$ for 10 min and (b) 10 mM (c) 20 mM (d) 40 mM $BaCl_2$ for 2 min. The structures were then kept in culture medium over 7 d.

24 h using $BaCl_2$ concentrations of 60 and 100 mM. Therefore based on the degradation results and MTT assay data, 60 mM of $BaCl_2$ was chosen as the tertiary cross-linking agent rather than 40 mM of $BaCl_2$ which could further enhance the alginate hydrogel stability and support cell growth within the alginate structure for at least 7 d or more as previously discovered.

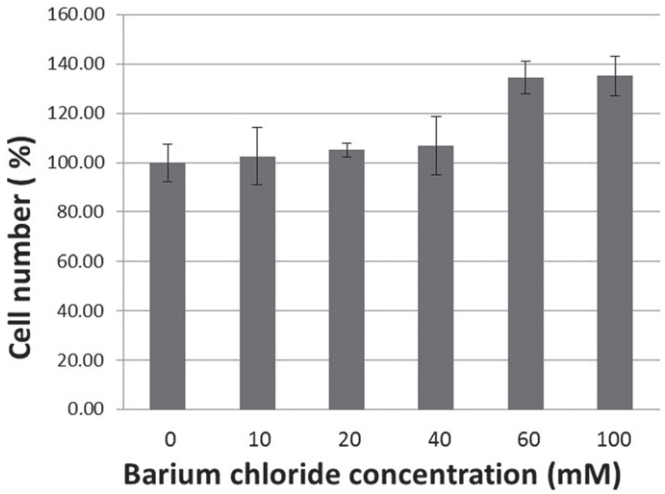

Figure 6. MTT Assay of U87-MG cells after 24 h of culture after being exposed 100 mM of $CaCl_2$ for 10 min and then exposed to different $BaCl_2$ concentrations.

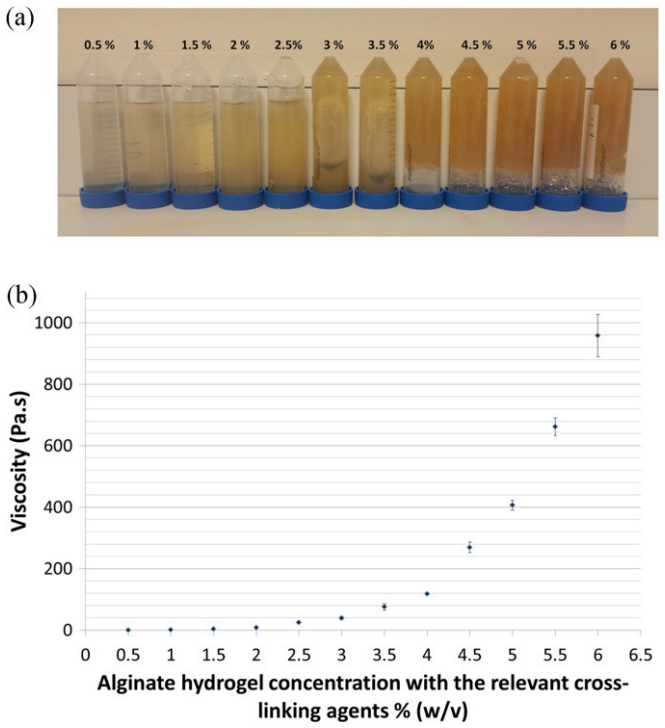

Figure 7. (a) Prepared partially cross-linked alginate hydrogels with their relevant cross-linking reagents in ascending order form left to right. (b) Partially cross-linked alginate hydrogel viscosity measurements.

3.6. The influence of the alginate viscosity on cell viability

The prepared partially cross-linked alginate hydrogels as shown in figure 7(a) had viscosity range from 0.13 ± 0.12 Pa.S at 0.5% to 958 ± 69 Pa.S at 6%. The viscosity increased exponentially in alginate hydrogel concentration as shown in figure 7(b). The hydrogel used in bioprinting which had a final alginate concentration of 4% (w/v) and $CaCl_2$ concentration of 40 mM had a viscosity of 117 ± 2.5 Pa.s. There appear to be a turning point in the viscosity change, which is around 4.0%. Additionally, the visual inspection of alginate in centrifuge tubes shows 4% is also the transitional point of alginate concentration where more solid hydrogel is formed.

Cell viability of bioprinted U87-MG cells shown in figure 8 indicates that, 2%, 3%, and 4% (w/v) partially cross-linked alginates with their relevant cross-linking reagents were maintained above 90% immediately after bioprinting. However cell viability of U87-MG cells dropped to 83.8% ± 1.2% due to a higher viscosity of the bio-ink when the concentration of partially

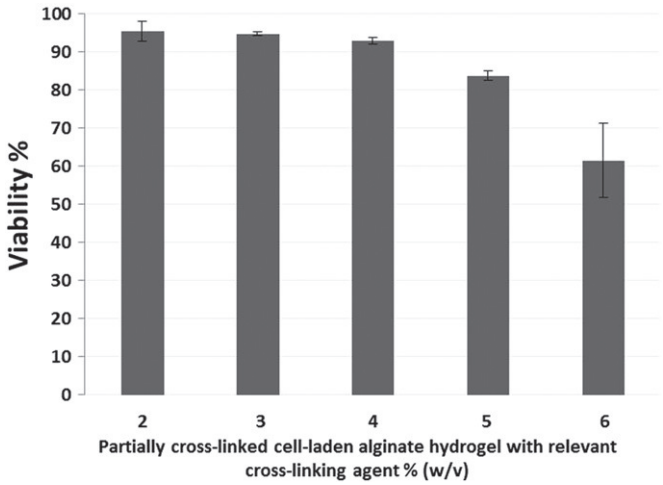

Figure 8. Cell viability of the bioprinted cell-laden partially cross-linked alginate hydrogel immediately after bioprinting at different concentrations.

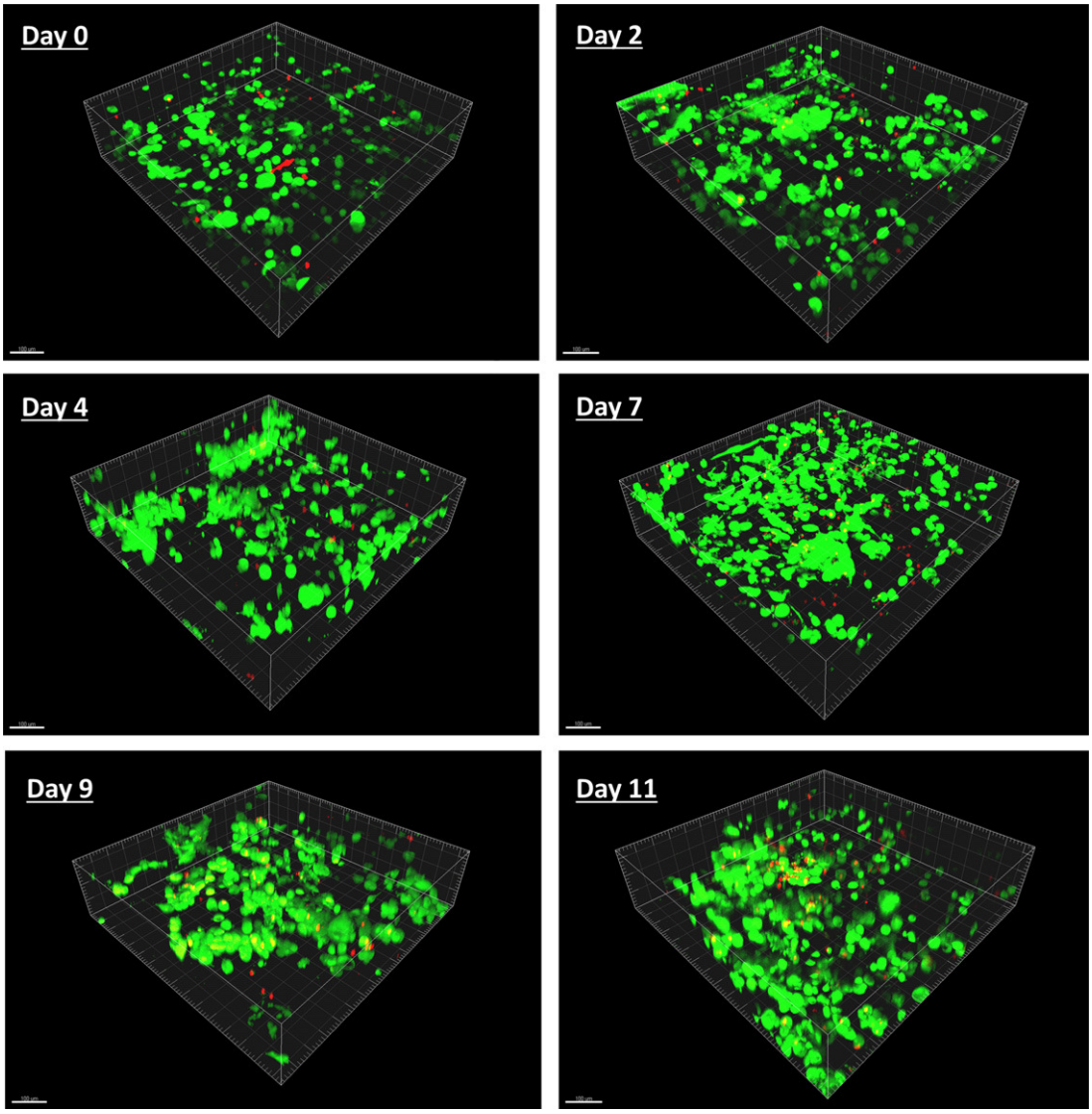

Figure 9. Confocal images of biopinted U87-MG cells throughout 11 d. The grid boxes are 50 μm, scale bar: 100 μm.

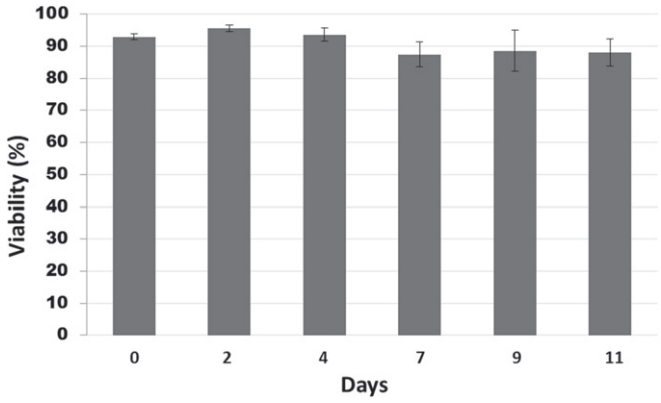

Figure 10. U87-MG Cell viability within 3D alginate hydrogel structures over the period of 11 d. Viability was assessed by choosing three random fields of the same construct.

cross-linked hydrogel was 5% compared to the lower concentrations. The cell viability in 6% partially cross-linked alginate hydrogel was 61.5% ± 9.8%, which was a dramatic change due to significant increase in viscosity of the hydrogel which was almost eight times higher than the normal printing condition of 4% partially cross-linked alginate hydrogel.

3.7. 3D printing of U87-MG cells in alginate hydrogel and its effect on cell Viability

U87-MG cells were bioprinted with partially cross-linked alginate hydrogel and then cross-linked with 100 mM $CaCl_2$ for 10 min followed by matrix stabilisation with 60 mM $BaCl_2$ for 2 min. Cell viability in the 3D constructs was monitored for 11 d post-printing as shown in confocal images in figure 9. Figure 10 summarised the 3D cell viability throughout the 11 d period. The printed cells had a viability of 92.9% ± 0.9% immediately after printing at day 0. Viability then remained steadily high, staying over 88% ± 4.3%. The cross-linked alginate hydrogel maintained its structure over 11 d while keeping the embedded cell viability over 88% ± 4.3% throughout which indicates a suitable permeability of the alginate hydrogel to allow efficient diffusion of nutrient, oxygen and waste removal within the alginate hydrogel. And as seen in figure 6 the U87-MG cells appear as individual cells immediately after printing, however within days of culture, proliferation through to the gel allows intercellular interaction implying a good porosity of the alginate hydrogel.

4. Conclusions

In this paper we developed a new bioprinting technique for 3D printing of alginate based hydrogel structures and evaluated its applicability for 3D bioprinting of tumour cells. Using this new free-form fabrication technique, partially cross-linked alginate hydrogels were formulated with tuneable mechanical properties to create tubular and more complex, and continuous 3D hydrogel structures. Degradation time of alginate hydrogel in cell culture media was investigated and the stability of the alginate hydrogel can be enhanced by post-printing treatment of $BaCl_2$. The proposed technique enables the possibility of bioprinting live human cells with high cell survival rate after bioprinting. This is a promising bioprinting technique that can be applied to fabricate clinically sized soft tissues with more complex and multi-cellular structures.

Acknowledgments

The authors acknowledge the funding support from the EPSRC (Grant No: EP/M506837/1), Innovate UK and NC3Rs (Advancing the development and application of non-animal technologies programme). AGT and MAH were supported by Heriot-Watt University scholarships. The authors would like to thank Dr Stephen Euston, Mr Paul Scanlan and Mr Javier Torralba (Heriot-Watt University) for the assistance in the rheology and mechanical measurement of hydrogels, Mr Christopher Mills (Edinburgh University) for Gama sterilization of sodium alginate used in this study.

References

[1] Mironov V, Trusk T, Kasyanov V, Little S, Swaja R and Markwald R 2009 Biofabrication: a 21st century manufacturing paradigm *Biofabrication* **1** 022001
[2] Wang C, Tang Z, Zhao Y, Yao R, Li L and Sun W 2014 Three-dimensional *in vitro* cancer models: a short review *Biofabrication* **6** 022001
[3] Huang G, Wang L, Wang S, Han Y, Wu J, Zhang Q, Xu F and Lu T J 2012 Engineering three-dimensional cell mechanical microenvironment with hydrogels *Biofabrication* **4** 042001
[4] Reiffel A J *et al* 2013 High-fidelity tissue engineering of patient-specific auricles for reconstruction of pediatric microtia and other auricular deformities *PLoS One* **8** e56506
[5] Boland T, Tao X, Damon B J, Manley B, Kesari P, Jalota S and Bhaduri S 2007 Drop-on-demand printing of cells and materials for designer tissue constructs *Mater. Sci. Eng.* C **27** 372–6

[6] Hollister S J 2005 Porous scaffold design for tissue engineering *Nat. Mater.* **4** 518–24
[7] Koch L *et al* 2012 Skin tissue generation by laser cell printing *Biotechnol. Bioeng.* **109** 1855–63
[8] Xu T, Binder K W, Albanna M Z, Dice D, Zhao W, Yoo J J and Atala A 2013 Hybrid printing of mechanically and biologically improved constructs for cartilage tissue engineering applications *Biofabrication* **5** 015001
[9] Arai K, Iwanaga S, Toda H, Genci C, Nishiyama Y and Nakamura M 2011 Three-dimensional inkjet biofabrication based on designed images *Biofabrication* **3** 034113
[10] Yamaguchi S, Ueno A, Akiyama Y and Morishima K 2012 Cell patterning through inkjet printing of one cell per droplet *Biofabrication* **4** 045005
[11] Xu T, Binder K W, Albanna M Z, Dice D, Zhao W, Yoo J J and Atala A 2013 Hybrid printing of mechanically and biologically improved constructs for cartilage tissue engineering applications *Biofabrication* **5** 015001
[12] Nishiyama Y, Nakamura M, Henmi C, Yamaguchi K, Mochizuki S, Nakagawa H and Takiura K 2008 Development of a three-dimensional bioprinter: construction of cell supporting structures using hydrogel and state-of-the-art inkjet technology *J. Biomech. Eng.* **131** 035001
[13] Cui X and Boland T 2009 Human microvasculature fabrication using thermal inkjet printing technology *Biomaterials* **30** 6221–7
[14] Kang K H, Hockaday L A and Butcher J T 2013 Quantitative optimization of solid freeform deposition of aqueous hydrogels *Biofabrication* **5** 035001
[15] Shim J-H, Kim J Y, Park M, Park J and Cho D-W 2011 Development of a hybrid scaffold with synthetic biomaterials and hydrogel using solid freeform fabrication technology *Biofabrication* **3** 034102
[16] Shim J-H, Lee J-S, Kim J Y and Cho D-W 2012 Bioprinting of a mechanically enhanced three-dimensional dual cell-laden construct for osteochondral tissue engineering using a multi-head tissue/organ building system *J. Micromech. Microeng.* **22** 085014
[17] Faulkner-Jones A, Greenhough S, King J A, Gardner J, Courtney A and Shu W 2013 Development of a valve-based cell printer for the formation of human embryonic stem cell spheroid aggregates *Biofabrication* **5** 015013
[18] Li C *et al* 2015 Rapid formation of a supramolecular polypeptide–DNA hydrogel for *in situ* three-dimensional multilayer bioprinting *Angew. Chem. Int. Ed.* **54** 3957–61
[19] Khalil S and Sun W 2009 Bioprinting endothelial cells with alginate for 3D tissue constructs *J. Biomech. Eng.* **131** 111002
[20] Faulkner-Jones A, Fyfe C, Cornelissen D J, Gardner J, King J, Courtney A and Shu W 2015 Bioprinting of human pluripotent stem cells and their directed differentiation into hepatocyte-like cells for the generation of mini-livers in 3D *Biofabrication* **7** 044102
[21] Ali M, Pages E, Ducom A, Fontaine A and Guillemot F 2014 Controlling laser-induced jet formation for bioprinting mesenchymal stem cells with high viability and high resolution *Biofabrication* **6** 045001
[22] Gudapati H, Yan J, Huang Y and Chrisey D B 2014 Alginate gelation-induced cell death during laser-assisted cell printing *Biofabrication* **6** 035022
[23] Gruene M, Pflaum M, Deiwick A, Koch L, Schlie S, Unger C, Wilhelmi M, Haverich A and Chichkov B N 2011 Adipogenic differentiation of laser-printed 3D tissue grafts consisting of human adipose-derived stem cells *Biofabrication* **3** 015005
[24] Ovsianikov A, Gruene M, Pflaum M, Koch L, Maiorana F, Wilhelmi M, Haverich A and Chichkov B 2010 Laser printing of cells into 3D scaffolds *Biofabrication* **2** 014104
[25] Guillotin B *et al* 2010 Laser assisted bioprinting of engineered tissue with high cell density and microscale organization *Biomaterials* **31** 7250–6
[26] Arcaute K, Mann B and Wicker R 2006 Stereolithography of three-dimensional bioactive poly(Ethylene Glycol) constructs with encapsulated cells *Ann. Biomed. Eng.* **34** 1429–41
[27] Censi R, Schuurman W, Malda J, di Dato G, Burgisser P E, Dhert W J A, van Nostrum C F, di Martino P, Vermonden T and Hennink W E 2011 A printable photopolymerizable thermosensitive p(HPMAm-lactate)-PEG hydrogel for tissue engineering *Adv. Funct. Mater.* **21** 1833–42
[28] Hockaday L A *et al* 2012 Rapid 3D printing of anatomically accurate and mechanically heterogeneous aortic valve hydrogel scaffolds *Biofabrication* **4** 035005
[29] Lee J-S, Hong J M, Jung J W, Shim J-H, Oh J-H and Cho D-W 2014 3D printing of composite tissue with complex shape applied to ear regeneration *Biofabrication* **6** 024103
[30] Campos D F D, Blaeser A, Weber M, Jäkel J, Neuss S, Jahnen-Dechent W and Fischer H 2013 Three-dimensional printing of stem cell-laden hydrogels submerged in a hydrophobic high-density fluid *Biofabrication* **5** 015003
[31] Zhao Y, Yao R, Ouyang L, Ding H, Zhang T, Zhang K, Cheng S and Sun W 2014 Three-dimensional printing of Hela cells for cervical tumor model *in vitro Biofabrication* **6** 035001
[32] Wang C, Tang Z, Zhao Y, Yao R, Li L and Sun W 2014 Three-dimensional *in vitro* cancer models: a short review *Biofabrication* **6** 022001
[33] Liliang O, Rui Y, Shuangshuang M, Xi C, Jie N and Wei S 2015 Three-dimensional bioprinting of embryonic stem cells directs highly uniform embryoid body formation *Biofabrication* **7** 044101
[34] Qian Y, Ma J, Guo X, Sun J, Yu Y, Cao B, Zhang L, Ding X, Huang J and Shao J F 2015 Curcumin enhances the radiosensitivity of U87 cells by inducing DUSP-2 up-regulation *Cell. Physiol. Biochem.* **3** 1381–93
[35] Kucharzewska P, Christianson H C, Welch J E, Svensson K J, Fredlund E, Ringnér M, Mörgelin M, Bourseau-Guilmain E, Bengzon J and Belting M 2013 'Exosomes reflect the hypoxic status of glioma cells and mediate hypoxia-dependent activation of vascular cells during tumor development *Proc. Natl Acad. Sci. USA* **110** 7312–7
[36] Diaz Miqueli A, Rolff J, Lemm M, Fichtner I, Perez R and Montero E 2009 Radiosensitisation of U87MG brain tumours by anti-epidermal growth factor receptor monoclonal antibodies *Br. J. Cancer* **100** 950–8
[37] Clark M J *et al* 2010 U87MG decoded: the genomic sequence of a cytogenetically aberrant human cancer cell line *PLoS Genetics* **6** e1000832
[38] Aleksander S, Zhang J, McCoard L, Xu X, Oottamasathien S and Prestwich G D 2010 *Tissue Eng.* A **16** 2675–85
[39] Daniel L C, Lo W, Tsavaris A, Peng D, Lipson H and Bonassar L J 2011 *Tissue Eng.* C **17** 239–48
[40] Tumbleston J R *et al* 2015 Continuous liquid interface production of 3D objects *Science* **347** 1349–52
[41] Mørch Ý A, Donati I and Strand B L 2006 Effect of Ca^{2+}, Ba^{2+}, and Sr^{2+} on alginate microbeads *Biomacromolecules* **7** 1471–80